Protection of Converter Interfaced Generation and Microgrids

Sakis Meliopoulos, *Fellow, IEEE*, George Cokkinides, *Member, IEEE*, Yu Liu, *Student Member, IEEE*, Rui Fan, *Student Member, IEEE*, Paul Myrda, *Member, IEEE*, Evangelos Farantatos, *Member, IEEE*

Abstract*— The protection of converter interfaced generation and associated circuits and components is challenging due to (a) insufficient separation between fault and load currents caused by converter interfaced sources, (b) large fault contributions from utility side – small fault contributions from inverter based sources and (c) requirement to operate in utility connected mode as well as islanded mode. These issues are common for wind systems, PV systems and μGrids. They are addressed with the proposed dynamic state Estimation Based Protection (EBP) method applied to each component of a converter interfaced system and associated components. The paper discusses the issues, presents the EBP method and the integration of the method with the inverter controls for the purpose of increasing the reliability of these systems. Several examples are provided which compare the proposed method with traditional protection functions.

***Index Terms*—Dynamic State Estimation (DSE), Converter Interfaced Generation (CIG), Quadratized Model, Algebraic Companion Form (ACF), Estimation Based Protection (EBP).**

I. Introduction

MODERN power systems are becoming increasingly complex as more converter interfaced generation (CIG) is added to the system in the form of wind, PV and μGrids. Protection must be reliable and fast to meet safety requirements and damage avoidance to these systems. Protection of CIG systems and μGrids is challenging with legacy protection functions for a number of reasons: (a) fault currents may be comparable to load currents, (b) disparity between fault currents from the power grid and from the CIG/μGrid side, (c) relatively small short circuit currents (weak sources) in wind farms and PV plants as well as in μGrids. In addition, converter systems may have complex control functions that create complex switching effects and interactions among inverters. The protection of power converter systems is required to distinguish between the abnormal operating conditions and the normal switching sequence and associated normal transients and waveform distortion. As renewable generation increases, protection challenges increase when legacy protection schemes are contemplated for these systems.

Converter interfaced generation (CIG) involves an inverter that may be capable of two way operation as the name implies. The inverter is equipped with sophisticated control circuits which control the firing of the solid state switches as well as perform higher level control functions such as ramping power, performing Low Voltage Ride-Through (LVRT) functions as well as protection functions. In such a system the protection and control functions cannot be separated as they are very tightly interlinked.

CIG systems, such as a WTS with a DFIG, the protection of the inverter often includes a separate crowbar [1] or dc chopper [2] that blocks the firing of switches when detection of overcurrent occurs. This protection is very fast and is necessary to protect the sensitive power electronic switches. This system should be integrated and coordinated with other control and protection functions for the proper operation and function of the system as: (a) low voltage ride through that requires the system to remain connected during a low voltage resulting from faults outside the CIG system and gradually restore real and reactive power when the fault is cleared [3], (b) continuous synchronization with the power grid as the voltage and frequency of the system changes gradually or abruptly due to external events, and (c) detect internal faults in the CIG system in which case the protection system should disconnect the CIG system.

During these transients, proper switching strategies are required to achieve short settling times [1], [4] that often induce transient currents that may create additional unintended protection issues. While solutions exist by adding additional equipment such as timing control of crowbar operation, application of a dynamic voltage restorer [5], use of a dynamic brake resistor [6], and other, it is recognized that coordination of protection and control functions may provide a better and more efficient approach.

Similar issues exist in μGrids: fault currents contributed by DG sources are much smaller than those contributed by the main grid. In addition, the μGrid network changes more frequently due to variable and intermittent generation. Traditional protection schemes for μGrids have many shortcomings. First, for overcurrent protection, the settings cannot be properly chosen, because: (a) fault currents are limited via power electronic devices, thus there is not enough separation between fault and load currents; (b) fault and operating currents differ according to the number of connected DG sources. Second, distance protection cannot securely and dependably operate because: (a) the μGrid circuits are usually

quite short, leading to limited selectivity of distance relays; (b) the effect of fault impedance is magnified by the imbalanced fault currents from main grid and DG sources leading to mis-operations.

Similar issues exist for solar photovoltaic (PV) systems since they are also interfaced to the system via inverters. Traditional systems use overcurrent devices for the protection of PV arrays [7]-[9]. However, the overcurrent device, which is typically a fuse, will be unable to detect the fault current during low irradiance because the level of the current is much lower than the operating range of the fuse. In addition, studies have shown that the presence of MPPT makes it more difficult to detect the fault currents [10], because the MPPT keeps the fault current lower when it operates to achieve the maximum power. Differential protection schemes have also been proposed [11]. However, it is possible for an internal fault shorting out a set of PV modules, the current going out of the array to be equal to that coming in. This type of fault would never be detected by the differential protection.

In summary, protection of CIG systems cannot be reliable achieved with conventional protection schemes. New protection schemes are required that will reliably protect these systems. We have introduced a new approach for protection of conventional power system protection zones based on dynamic state estimation [14], [15]. In this paper, we discuss the suitability of the method to the protection needs of CIG systems such as WTS, PV farms and μGrids. We provide a brief summary of the method, followed by its application to CIG systems.

II. Proposed Method

A brief review of the proposed approach for protection of converter interfaced generators (CIG) systems is provided.

A. Overview of the Proposed Approach

The dynamic state estimation based protection has been inspired from the differential protection function and can be considered as an extension and generalization of the differential protection function.

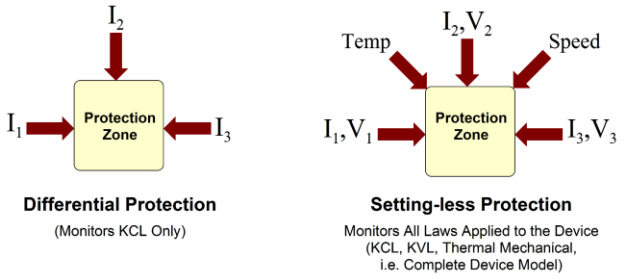

Figure 1: Evolution of the Differential Protection Function [15]

Specifically, the differential protection function monitors Kirchoff's current law for a protection zone, i.e. the sum of currents into the zone must equal zero. We extend this concept as follows. If measurements of various quantities in a protection zone are taken, all the measurements must satisfy the dynamic model of the protection zone, as long as the protection zone does not experience a fault condition. A systematic way to determine whether the measurements satisfy the dynamic model of the protection zone is by means of dynamic state estimation. The application of dynamic state estimation in this case requires the dynamic model of the protection zone, the model of the measurements and the dynamic state estimation algorithms. A flow chart of the approach is shown in Figure 2.

The method requires the following, as can be seen in Figure 2: (a) the dynamic model of the protected component; (b) Dynamic State Estimation process to test the consistency between the measurements and the dynamic model; (c) trip logic of the relay. These steps are discussed next.

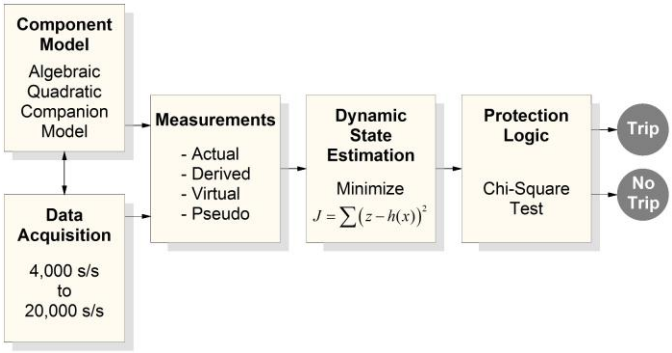

Figure 2: Dynamic State Estimation Based Protection Method

B. Dynamic Model of the Protected Component

The dynamic model of the protected component consists of a set of differential and algebraic equations. We have also proposed a quadratization method to reduce all high order nonlinearities of a device model, if present, to second order or less by introducing additional variables. The resulting quadratized dynamic model (QDM) is abstracted into an object of a specific standard syntax. The resulting object-oriented model leads to standardization of the analytics of the protection method for any component (zone). The syntax of the QDM is:

$$\begin{aligned} i(t) &= Y_{eqx1}\mathbf{x}(t) + D_{eqxd1}\frac{d\mathbf{x}(t)}{dt} + C_{eqc1} \\ 0 &= Y_{eqx2}\mathbf{x}(t) + D_{eqxd2}\frac{d\mathbf{x}(t)}{dt} + C_{eqc2} \\ 0 &= Y_{eqx3}\mathbf{x}(t) + \left\{ \begin{array}{c} \vdots \\ \mathbf{x}(t)^T \left\langle F^i_{eqxx3} \right\rangle \mathbf{x}(t) \\ \vdots \end{array} \right\} + C_{eqc3} \end{aligned} \quad (1)$$

And measurements:

$$\mathbf{z}(\mathbf{x}) = Y_{mx}\mathbf{x}(t) + \left\{ \begin{array}{c} \vdots \\ \mathbf{x}(t)^T \left\langle F^i_{mx} \right\rangle \mathbf{x}(t) \\ \vdots \end{array} \right\} + D_{mx}\frac{d\mathbf{x}(t)}{dt} + C_m + \eta(t) \quad (2)$$

where $i(t)$ are through variables (for most devices terminal currents); $\mathbf{x}(t)$ are state variables, $z(t)$ are measurements, $\eta(t)$ are measurement errors. The other elements of the model are parameter matrices and vectors of the specific component.

C. Dynamic State Estimation Process

A mathematically rigorous and systematic method to test the consistency between the measurements and the model, is by

means of the Dynamic State Estimation. For this application, we convert the dynamical equations into discrete time equations via the quadratic integration method yielding the Algebraic Quadratic Companion Form (AQCF). Note that the AQCF include variables at both time t and t_m and past history terms at time *t-h*, where h is the time step and t_m is the mid-point of the time interval [t-h,t]. The syntax of the AQCF is:

$$\begin{Bmatrix} i(t) \\ 0 \\ 0 \\ i(t_m) \\ 0 \\ 0 \end{Bmatrix} = Y_{eqx}\mathbf{x}(t,t_m) + \begin{Bmatrix} \vdots \\ \mathbf{x}(t,t_m)^T \left\langle F_{eqx}^i \right\rangle \mathbf{x}(t,t_m) \\ \vdots \end{Bmatrix} + b\left(t-h\right) \quad (3)$$

$$z(\mathbf{x}) = Y_{eqx}\mathbf{x}(t,t_m) + \begin{Bmatrix} \vdots \\ \mathbf{x}(t,t_m)^T \left\langle F_{eqx}^i \right\rangle \mathbf{x}(t,t_m) \\ \vdots \end{Bmatrix} + b_z\left(t-h\right) + \eta\left(t,t_m\right) \quad (4)$$

Additional information for the object-oriented modeling approach can be found in [17].

The dynamic state estimation can be performed by a number of well-developed methods (unconstraint weighted least squares approach, constraint weighted least squares approach, Extended Kalman filter and others). In this case, we use the unconstraint weighted least squares approach (WLS). The WLS basic solves the following optimization problem:

$$\begin{aligned} &Minimize \quad J(\mathbf{x}) = \eta^T(t,t_m)\eta(t,t_m) \\ &= \left(Y_{eqx}\mathbf{x}(t,t_m) + \begin{Bmatrix} \vdots \\ \mathbf{x}(t,t_m)^T \left\langle F_{eqx}^i \right\rangle \mathbf{x}(t,t_m) \\ \vdots \end{Bmatrix} + b_z\left(t-h\right) - z(\mathbf{x}) \right)^T \\ &W \left(Y_{eqx}\mathbf{x}(t,t_m) + \begin{Bmatrix} \vdots \\ \mathbf{x}(t,t_m)^T \left\langle F_{eqx}^i \right\rangle \mathbf{x}(t,t_m) \\ \vdots \end{Bmatrix} + b_z\left(t-h\right) - z(\mathbf{x}) \right) \end{aligned} \quad (5)$$

where $\mathbf{W} = \text{diag}\left\{\cdots, 1/\sigma_i^2, \cdots\right\}$ and σ_i is the standard deviation of the measurement error.

The solution of the above optimization problem is given with the following iterative algorithm:

$$\begin{aligned} &\mathbf{x}^{\nu+1} = \mathbf{x}^{\nu} - (H^T W H)^{-1} H^T W \\ &\left(Y_{eqx}\mathbf{x}^{\nu}(t,t_m) + \begin{Bmatrix} \vdots \\ \mathbf{x}^{\nu}(t,t_m)^T \left\langle F_{eqx}^i \right\rangle \mathbf{x}^{\nu}(t,t_m) \\ \vdots \end{Bmatrix} + b_z\left(t-h\right) - z(\mathbf{x}^{\nu}) \right) \end{aligned} \quad (6)$$

where *H* is the Jacobean matrix:

$$H = Y_{m,x} + \begin{Bmatrix} \vdots \\ \left(\mathbf{x}^{\nu}\right)^T F_{m,x}^i + F_{m,x}^i\left(\mathbf{x}^{\nu}\right) \\ \vdots \end{Bmatrix} \quad (7)$$

D. Relay Trip Logic

The consistency between the measurements and the model is tested by examining whether the residuals of the Dynamic State Estimation (the differences between the actual and the estimated measurements) is comparable to the meter accuracy by which the measurement were taken. If the errors are much larger than the metering errors, we can conclude that the component model has changed and there must be an internal fault. A systematic way to quantify this comparison is to use the chi-square test [14], where the confidence level $p(t)$ is calculated by:

$$p(t) = P\left(\chi^2 \geq J\left(\hat{\mathbf{x}}\right)\right) = 1 - P\left(J\left(\hat{\mathbf{x}}\right), \nu\right) \quad (11)$$

where $P\left(J\left(\hat{\mathbf{x}}\right), \nu\right)$ is the probability of χ^2 distribution of $\chi^2 \leq J\left(\hat{\mathbf{x}}\right)$, with ν degree of freedom. $\hat{\mathbf{x}}$ is the estimated states of the component.

A high confidence level (near 100%) suggest that the measurements fit the model quite well. If the confidence level is low or oscillating, we can conclude that an internal fault happened inside the component and the relay should trip this component. As a matter of fact we use the results of the chi square test to detect (targets) faults and to decide the trip time with the following algorithm. In general three settings are used. The first setting defines how the method asserts a fault. If the confidence level is less than 0.2 for *N* consecutive estimations, the fault target is set. N is a user selected setting. We recommend a default value of 2. The next two settings are the reset time (T_r) and the delay time (T_d) of the method. The trip decision is made when the following condition is satisfied:

$$\int_{t-T_r}^{t} \left(1 - p\left(\tau\right)\right) d\tau > T_d$$

Where t is the present time. Note that in general when the confidence level goes to zero for duration equal to T_d the method will trip the protection zone.

III. Illustrative Results – Zone Protection

The proposed method is demonstrated with two example systems. The first one is a μGrid and the second is a Wind Turbine System connected to the power grid with a transmission circuit. The first example is used to compare the performance of the proposed method with legacy protection functions as applied to a μGrid. The second example demonstrates the seamless integration of the proposed protection method with the inverter controls of a WTS for stable operation of the WTS during transient events in and around the system.

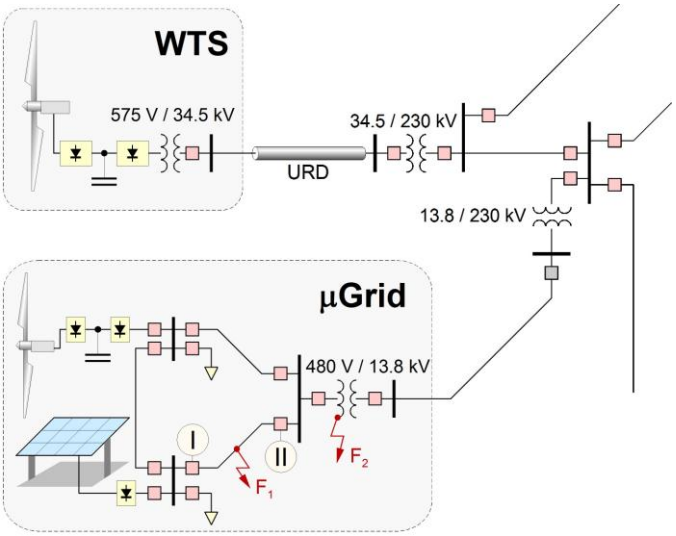

Figure 3: Example Test System

A. *Description of Example System*

The example system is shown in Figure 3. The µGrid is connected to a 13.8 kV distribution system via a 750 kVA, 13.8kV/480V transformer. The point of common coupling is at the high side of this transformer. A 13.8 kV solid state switch is located at the point of common coupling. The power grid consists of distribution and transmission circuits as indicated in the figure. The power grid also includes a type 4 WTS system which consists of wind turbines, converters and a 34.5kV/575V transformer. The WTS system is connected to the transmission system via a 34.5 kV URD cable and a 230kV/34.5 kV transformer. The µGrid includes a 75 kW PV system operated at 600V DC which is connected via a 100 kVA, 600VDC/480V inverter. It also includes a small 25 kVA wind turbine system of type 4. Each component in the system is represented with a model in the SCAQCF script. Each component constitutes a protection zone. For demonstration purposes, two events are considered and discussed.

B. *Results – Event 1*

A phase A to neutral fault occurs at a certain time in the 480V µGrid circuit I-II, location F_1, as shown in Figure 3. The location F_1 is at 48% of the circuit length from terminal II of the I-II circuit. The configuration of circuit I-II is shown in Figure 4. The circuit parameters are given in Table 1. To test the performance of the distance relay (legacy protection), we demonstrate a fault at location F_1 of the protected circuit I-II. The fault impedance is 0.04 ohms. For this fault, the contribution to the fault current from side II (strong source) is much stronger than the contribution from side I (weak source).

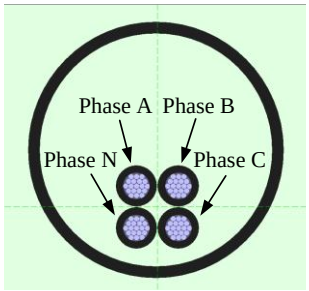

Figure 4. Circuit I-II Construction

Table 1: Example µGrid circuit parameters

Object	*Parameter*	*Value*
System	Line to line voltage	480 V
	Fundamental frequency	60 Hz
	Length of the monitored circuit	375 feet
Monitored Circuit	Positive (Negative) sequence	0.0957+ j 0.0153 Ω
	Zero sequence	0.2186+ j 0.1555 Ω

This system has been simulated for the described fault condition. The simulation results are shown in the first set of traces in Figure 6. Only the three phase currents are shown on the side II of the circuit. We examine the performance of the distance relay as well as the performance of the proposed EBP relay and compare the results.

The performance of the distance relay II in shown in Figure 5. The impedance "seen" by the relay superimposed on the characteristics of the relay are depicted in Figure 5. Here the settings of zone 1, 2 and 3 are 80%, 125% and 260% of the circuit positive impedance, respectively. We can clearly observe the following: The impedance "seen" by the distance relay already falls outside of zone 1 of the relay even if the relay setting is supposed to cover 80% of the circuit length and the fault is at 48% of the circuit length. This represents an almost 80% error in determining the location of the fault. This error is due to the fault impedance, the short length of the circuit and the inherent imbalance of the circuit. This error results in mis-operation of the relay.

The dynamic state estimation based protective relay uses three phase current and voltage measurements at both sides of the protected circuit I-II. The results are given in Figure 6. The first four sets of traces represent actual values, estimated values, residuals, and normalized residuals of currents at side II. The last two channels provide the confidence level and trip signal of the relay. We can observe that, the residuals are quite small during un-faulted conditions, and significant during the internal fault. The confidence level drops from 100% to 0% at time 1.4s, i.e. immediately after the inception of the internal fault.

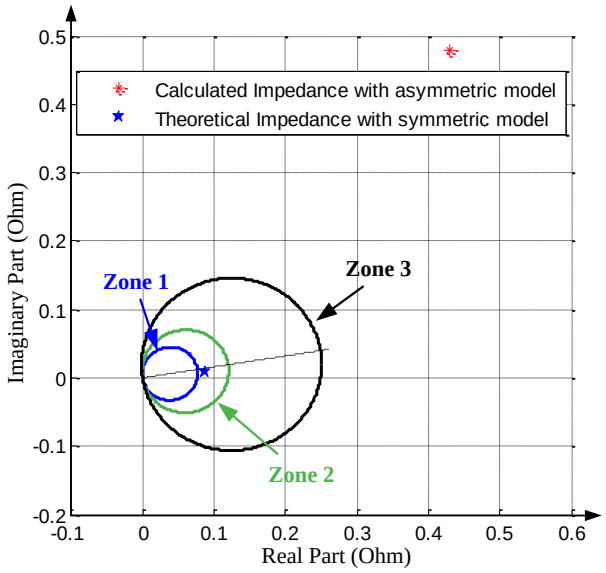

Figure 5. Distance Relay Characteristics

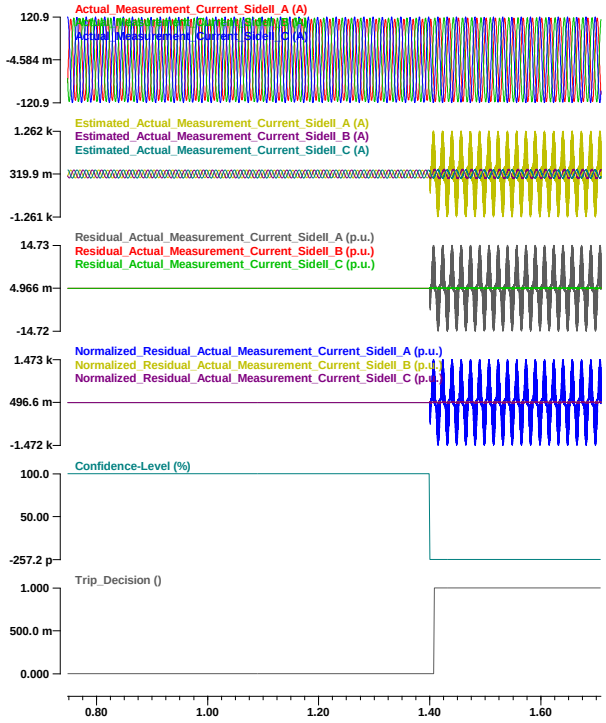

Figure 6. Phase A-N Internal Fault at 1.4s

This example shows that in this case the distance protection, a well defined and relatively reliable legacy protection function, failed to detect an internal fault in the correct zone. The proposed method reliably detected the fault condition. The speed of detection was less than one msec.

C. Results – Event 2

The protection zone under consideration is the 750 kVA, 480V/13.8kV delta-wye connected three-phase transformer, as shown in Figure 3. At time t = 6.5s, an internal low side (480V) phase A winding to ground fault occurs at a location of the winding which is 5% from the neutral of the transformer. The position of the fault is shown as F_2 in Figure 3.

A percentage differential protection scheme has been implemented to protect this transformer with the following settings (on the transformer side): pickup operating current of 2 A and 20% percentage ratio. The performance of the percentage differential relay for this fault event is shown in Figure 7. Note that the operating current is 1.5 A (less than 2 A) and the percentage ratio is 7.78% (less than 20%). Thus in this case the differential protection will not "see" the fault.

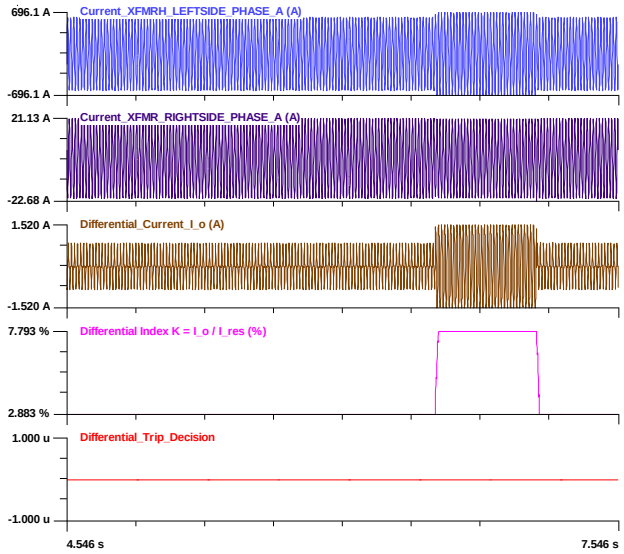

Figure 7: Results of the Differential Protection Scheme

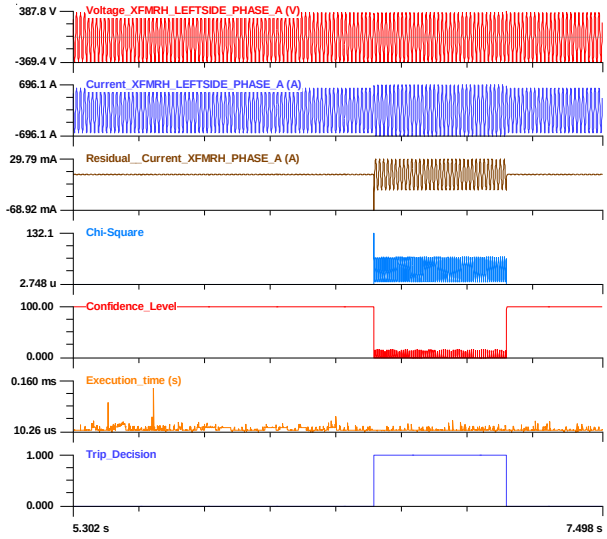

Figure 8: 5% Internal Turn-Ground Fault of Transformer

The performance of the EBP relay for this fault event is shown in Figure 8. Prior to the fault (normal operating conditions) the residual and chi-square values are very small and the confidence level stays at 100%. When this internal fault occurs the transformer voltages and currents are experiencing small changes. However, the chi-square values increase drastically and the confidence level drops from 100% to zero immediately. The EBP relay issues a trip command to protect the transformer.

The above example shows a case where a legacy differential protection function failed to detect an internal fault close to the neutral of the transformer. The dynamic state estimation based protective relay correctly identified the fault in time less than one msec.

IV. Integration of Protection & Control

Traditionally, power electronic based devices and systems have sophisticated controls which also integrate protection functions via software and hardware. For utility size wind, PV

and μGrids, there is also the requirement of low voltage ride through (LVRT) function which is achieved via an integrated protection and control system. One of the issues facing CIG systems is the fact that during frequency swings of the power grid the inverter controller may not be able to keep up with the continuous changing of the frequency and may result in transients that will force shutting down the inverter. The DSE based protection method has the capability to integrate with the control loops of the power electronics of CIGs and to improve the performance of the power electronic subsystems during these transients. We propose integration of protection and control in power electronic subsystems supervised by the dynamic state estimation based protection system. The integration is demonstrated with an example.

V. Illustrative Results – CIG Protection & Control

The protection and control functions are intertwined in CIG systems, i.e. systems that include power electronic subsystems, such as wind turbines/generators/inverters, or PV/inverters, etc. When CIG is attached to the power grid, any transients and power system oscillations will affect the operation of the CIG subsystem as well as its operation and protection. Because the safe operating region of inverters is very small (tight margins), it is important to minimize transients and any disturbances from reaching the inverter. For example, one protection mechanism for the inverter is to stop operation when the disturbance is such that affect the proper switching of the electronic valves of the inverter. It is important in this case to utilize the protection system to provide additional information to the inverter controller to minimize switching transients or the keep the inverter in synchronism with the power system. We use the dynamic state estimation method to provide transient and system trajectory information to the inverter controller so that it will operate in synchronism with the system and avoid transients that will cause the tripping of the inverter. This approach will be illustrated with an example test system. The approach integrates inverter controls and the proposed protection method; specifically the proposed protection method provides signals to the inverter controller (specifically frequency and rate of frequency change) which are used for supplementary (predictive) controls of the inverter. The test system consists of a wind turbine system that is connected to the power grid via a transmission line as illustrated in Figure 9.

Note that the EBP relay estimates the frequency and rate of change of frequency locally and at the other end of the transmission circuit, i.e. the system using only local measurements and therefore without appreciable time latencies. Specifically, this is done by using only local measurements and a model that includes the inverter, transformer and the transmission line. The frequency and rate of change of frequency (locally and remotely) are provided to the inverter control as supplementary feedback signals. These signals are applied through a PID controller to the inverter controller enabling predictive control, i.e. the inverter anticipates the motion (oscillation) of the power system and adjusts the switching frequency so that the inverter always operates in synchronism with the power grid. The details are provided in reference [18]. We simply show typical results in Figure 10 for the system of Figure 9. The top two traces of Figure 10 show the real and reactive power of the inverter without the supplementary controls from the EBP relay (DSE Based Protection), while traces 3 and 4 with these controls.

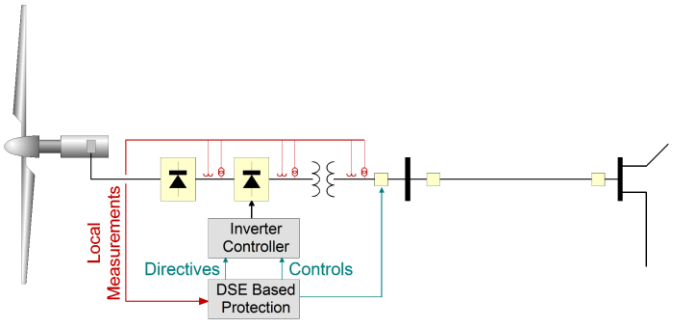

Figure 9: Example of CIG Integrated Protection and Control

Note that without the integrated protection and control, the inverter output oscillates while with the integrated system, the inverter output is practically constant.

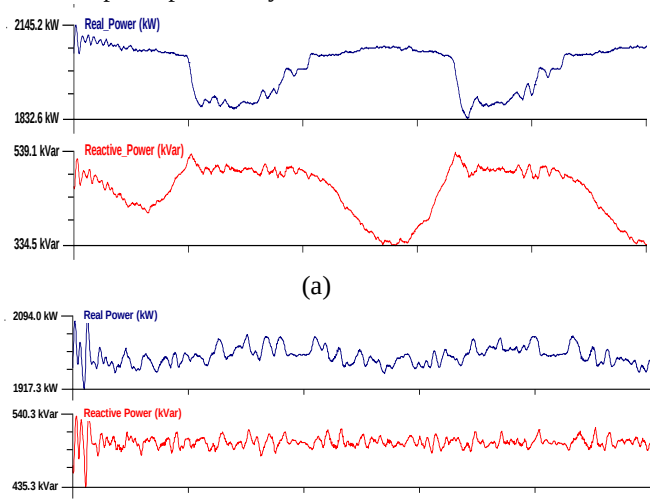

Figure 10: Inverter Real and Reactive Power during a Disturbance
Without Integrated Protection & Control (a), with proposed system (b)

Above example shows the ability of the integrated protection and control system to synchronize the operation of the WTS in the presence of a system disturbance (resulting in an oscillation of the system). This ability drastically minimizes the possibility of the WTS needing to recall low voltage ride-through during disturbances and drastically maximizes the reliability of the system. In case of a fault, the proposed system will identify the fault as it has been shown in other examples and it will initiate the correct protection action.

Note that the information that the EBP relay provides, can be used in the anti-islanding schemes. As a matter of fact, the above example shows that by continuously synchronizing the inverter to the system motion (oscillations, disturbances) the need to island the system is diminished. Obviously this is an important issue that is under investigation and we will report in subsequent papers. It is pointed out that the LVRT and anti-islanding schemes are interrelated and the integration of the EBP relay with these control schemes will result in

improved performance.

VI. Conclusions

A new EBP relay is presented with applications to systems with converter interfaced generation, such as wind systems, PV farms and μGrids. The proposed method naturally integrates with the control system of the inverter of these systems for improved reliability of the overall system. Several examples have been presented and compared to traditional protection schemes. The examples were selected to show that traditional protection schemes may fail while the proposed method is reliable and robust for the same events. To emphasize these points, examples were selected where legacy protection systems fail while the EBP approach reliably detects and identifies the fault conditions.

The EBP relay uses traditional relay instrumentation; preferably it can also use merging units and a process bus, i.e. can be attached to the process bus. It uses sampled values of voltages and currents and the dynamic state estimation is performed with the sampled values. For this reason, it detects faults in less than one msec, much faster than any known legacy relay. Present technology can extract sampled values and present them to the computer of the EBP with minimum latencies in the order of few microseconds. We have also proved in the laboratory that the analytics of the EBP can be performed within the typical sampling period of present day relay data acquisition systems. The end result is that the time latencies involved are less than typically 200 microseconds, most of it is the analytics of the relay.

The EBP relay requires a high fidelity model of the component under protection. For many power components we have accurate (high fidelity) models. The dynamic state estimation can also provide a measure of how accurate the model is. At the same time the dynamic state estimation can be also used to fine tune the parameters of the model so that it becomes a high fidelity model. For this purpose the parameters of the model are treated as unknown states to be estimated by the dynamic state estimation. We have performed this approach to a hydro generator with great success [17].

References

[1] J. Liang, D. Howard, J. Restrepo, R. Harley, "Feedforward transient compensation control for DFIG wind turbines during both balanced and unbalanced grid disturbances", IEEE Trans. on Industry Applications, vol. 49, no. 3, May 2013, pp. 1452-1463

[2] G. Pannell, B. Zahawi, D. Atkinson, P. Missailidis, "Evaluation of the performance of a DC-Link brake chopper as a DFIG low-voltage fault-ride-through device", IEEE Trans. on Energy Conversion, vol. 28, no. 3, Sep 2013, pp. 535-542

[3] C. Sourkounis, P. Tourou, "Grid code requirements for wind power integration in Europe", Hindawi Publishing Corporation, vol. 2013, Available Online: http://dx.doi.org/10.1155/2013/437674

[4] D. Xie, Z. Xu, "A Comprehensive LVRT Control Strategy for DFIG Wind Turbines With Enhanced Reactive Power Support", IEEE Trans. On Power Systems, vol. 28, no. 3, Aug 2013, pp 3302-3310..

[5] C. Wessels, F. Gebhardt, F. Fuchs, "Fault ride-through of a DFIG wind turbine using a dynamic voltage restorer during symmetrical and asymmetrical grid faults", IEEE Trans. on Power Electronics, vol. 26, no. 3, Mar 2011, pp. 807-815

[6] J. Yang, J. Fletcher, J. Reilly, "A Series-dynamic-resistor-based converter protection scheme for doubly-fed induction generator during various fault conditions", IEEE Trans. on Energy Conversion, vol. 25, no. 2, Jun 2010, pp. 422-432

[7] L. Bin, Y. Yue, W. Lei, "Research on Relay Protection of Grid-Connected Photovoltaic Power Station in the Plateau", *International Conference on Advanced Power System Automation and Protection*, Volume 3, pp. 1814-1818, 2011

[8] D. Collier, T. Key, "Electrical Fault Protection for a Large Photovoltaic Power Plant Inverter ", *IEEE Photovoltaic Specialists Conference*, pp. 1035-1042, 1988

[9] Y. Zhao, B. Lehman, J.-F de Palmer, J. Mosesian, R. Lyons, "Challenges to Overrcurrent Protection Devices under Line-Line Faults in Solar Photovoltaic Arrays," *IEEE Energy Conversion Congress and Exposition*, pp.20-27, 2011

[10] Y. Zhao, B. Lehman, J.-F de Palmer, J. Mosesian, R. Lyons, "Line-Line Fault Analysis and Protection Challenges in Solar Photovoltaic Array," to Overrcurrent Protection Devices under Line-Line Faults in Solar Photovoltaic Arrays," *IEEE transactions on Industrial Electronics*, Volume pp., Issue 99, 2012

[11] M. Nthontho, S.P Chowdhury, S. Winberg, S. Chowdhury, "Protection of Domestic Solar Photovoltaic Based Microgrid," *11th International Conference on Developments in Power Systems Protection*, 2012

[12] S. Durand, D. Bowling, V. Risser, "Lessons Learned From Testing Utility Connected PV Systems," *11st IEEE Photovoltaic Specialist Conference*, vol. 2, pp. 909-913, 1990

[13] W. Bower, J. Wiles, "Investigation of Ground-Fault Protection Devices for Photovoltaic Power Systems Applications," *28th IEEE Photovoltaic Specialist Conference*, pp. 1378-1383, 2000.

[14] A. P. Meliopoulos, G. J. Cokkinides, Z. Tan, S. Choi, Y. Lee, and P. Myrda, "Setting-less protection: Feasibility study," in *Proceeding of 2013 46th Hawaii International Conference on System Sciences (HICSS)*, Maui, HI, USA, Jan. 2013, pp. 2345–2353.

[15] Paul Myrda, Sakis Meliopoulos and George Cokkinides, "Dynamic State Estimation Based Protection: Laboratory Validation", Proceedings CIGRE USNC Grid of the Future Symposium, Houston, TX, October 19-21, 2014.

[16] Meliopoulos, A. P., Cokkinides, G., Rui Fan, Renke Huang, Yonghee Lee, Liangyi Sun, Zhenyu Tan "Setting-less Protection: Laboratory Testing", PSERC Publication 14-03, June 2014.

[17] Sakis (A.P.) Meliopoulos, George Cokkinides, Renke, Huang, Evangelos Farantatos, Bruce Fardanesh, George Stefopoulos, Clinton Hedrington, "Distributed Dynamic State Estimator, Generator Parameter Estimation and Stability Monitoring Demonstration", December 31, 2013.

[18] PSERC Report, Sakis Meliopoulos, "Hybrid Time Domain Simulation: Application to Protection and Control of Converter Interfaced Generation", December 2016.